Diagn Interv Radiol 2026; DOI: 10.4274/dir.2026.264340

CARDIOVASCULAR IMAGING

ORIGINAL ARTICLE

Association of cardiac magnetic resonance imaging parameters with N-terminal pro-B-type natriuretic peptide levels

İffet Doğan[1]
Kemal Buğra Memis[2]
Defne Şahin[3]
Önder Durmaz[2]
Serhat Hayme[4]
Mecit Kantarcı[2,5]

[1]University of Health Sciences Türkiye, Mehmet Akif Ersoy Thoracic and Cardiovascular Surgery Training and Research Hospital, Clinic of Radiology, İstanbul, Türkiye

[2]Erzincan Binali Yıldırım University Faculty of Medicine, Department of Radiology, Erzincan, Türkiye

[3]Bezmialem Vakif University Faculty of Medicine, Department of Diagnostic and Interventional Radiology, İstanbul, Türkiye

[4]Erzincan Binali Yıldırım University Faculty of Medicine, Department of Biostatistics and Medical Informatics, Erzincan, Türkiye

[5]Atatürk University Faculty of Medicine, Department of Radiology, Erzurum, Türkiye

PURPOSE

This study aimed to evaluate the associations between serum N-terminal pro-B-type natriuretic peptide (NT-proBNP) levels and conventional and tissue-characterization cardiac magnetic resonance (CMR) imaging parameters.

METHODS

This retrospective, single-center study included 204 patients who underwent CMR and had NT-proBNP measured within 7 days before or after the examination. Patients were categorized into three groups based on NT-proBNP levels: normal (< 125 pg/mL), high (125–500 pg/mL), and extremely high (> 500 pg/mL). A comparison of CMR-derived structural and functional parameters, including left ventricular ejection fraction, myocardial mass, left atrial (LA) diameter, late gadolinium enhancement (LGE), extracellular volume (ECV), and short tau inversion recovery (STIR)-based T2 signal-intensity (SI) ratio, was performed across groups. Associations were assessed using ordinal and multinomial logistic regression analyses.

RESULTS

Higher NT-proBNP levels were associated with increased myocardial mass, wall thickness, LA enlargement, and reduced systolic function. The LGE burden, LA cavity diameter, and ECV increased significantly across NT-proBNP groups. In adjusted multinomial logistic regression, the ECV and LA cavity diameter were independently associated with both the high and extremely high NT-proBNP groups. The STIR-based T2 SI ratio demonstrated an inverse association with NT-proBNP; however, an independent association was observed only in the extremely high NT-proBNP group (adjusted odds ratio: 0.80, $P = 0.034$), and this finding should be considered exploratory.

CONCLUSION

Higher NT-proBNP categories were associated with greater structural abnormalities and tissue-characterization changes on CMR, particularly a higher ECV and larger LA diameter. The inverse association observed with the STIR-based T2 SI ratio was limited to the extremely high NT-proBNP group and should be considered exploratory.

CLINICAL SIGNIFICANCE

Elevated NT-proBNP levels were associated with CMR findings consistent with myocardial remodeling, particularly increased ECV expansion.

KEYWORDS

Cardiac magnetic resonance, extracellular volume, late gadolinium enhancement, T2 signal-intensity ratio, myocardial remodeling, heart failure

Handling editor: Serçin Özkök

Corresponding author: Mecit Kantarcı

E-mail: akkanrad@hotmail.com

Received 23 July 2026; revision requested 05 August 2026; last revision requested 17 August 2026; accepted 19 August 2026.

Epub: 26.08.2026

DOI: 10.4274/dir.2026.264340

You may cite this article as: Doğan İ, Memis KB, Şahin D, Durmaz Ö, Hayme S, Kantarcı M. Association of cardiac magnetic resonance imaging parameters with N-terminal pro-B-type natriuretic peptide levels. *Diagn Interv Radiol*. 26 August 2026 DOI: 10.4274/dir.2026.264340 [Epub Ahead of Print].

The N-terminal pro-B-type natriuretic peptide (NT-proBNP) protein is released in response to increased myocardial wall stress and is widely used in the clinical evaluation of suspected heart failure (HF). However, elevated NT-proBNP is not specific to HF and may occur in various structural and functional cardiac disorders. Its concentration is also influenced by age, renal function, cardiac rhythm, and volume status. Therefore, patients referred for cardiac magnetic resonance (CMR) may demonstrate a broad range of NT-proBNP levels without necessarily fulfilling the clinical criteria for HF.[1-3]

For analytical purposes, NT-proBNP levels were categorized as normal (< 125 pg/mL), high (125–500 pg/mL), and extremely high (> 500 pg/mL). The threshold of 125 pg/mL was selected based on the established non-acute rule-out threshold for HF.[4] The 500 pg/mL cut-off was prespecified to distinguish modest elevations, previously described within the range of 125–500 pg/mL, from more marked elevations.[5,6] This threshold was used for analytical stratification and should not be interpreted as a universal diagnostic or prognostic cut-off.

CMR provides comprehensive assessment of cardiac morphology, ventricular function, and myocardial tissue characteristics across a wide range of cardiovascular diseases.[7,8] In addition to conventional parameters, late gadolinium enhancement (LGE), extracellular volume (ECV), and T2-weighted imaging may provide information regarding focal and diffuse myocardial abnormalities.[9] Nevertheless, the associations between NT-proBNP levels and these CMR parameters in a heterogeneous clinical CMR population remain incompletely characterized.[10,11]

Main points

- Increased N-terminal pro-B-type natriuretic peptide (NT-proBNP) levels correlate with the advancing structural and functional abnormalities observed in cardiac magnetic resonance imaging.
- Both late gadolinium enhancement and extracellular volume (ECV) increase across NT-proBNP categories, indicating progressive myocardial remodeling.
- ECV was independently associated with both the high and extremely high NT-proBNP categories.
- The short tau inversion recovery-based T2 signal-intensity ratio showed an association with NT-proBNP levels but requires further validation before clinical application.

The objective of this study is to evaluate the variations in basic and advanced CMR findings across three patient cohorts categorized by their serum NT-proBNP levels (normal/high/extremely high) and to ascertain the structural and functional CMR parameters associated with serum NT-proBNP levels.

Methods

Ethical approval

This study received ethical approval from the Clinical Research Ethics Committee at Erzincan Binali Yıldırım University (protocol number: 2026-06/12, date: 26.03.2026). The study involved a retrospective analysis of existing anonymized clinical and imaging data; since it did not require any additional intervention, written informed consent was waived. The study was conducted in accordance with the principles of the Declaration of Helsinki.

Study population

All adult patients who received CMR imaging at our medical center between January 1, 2024, and February 1, 2026, were retrospectively evaluated. The inclusion criteria for our study encompassed the detection of serum NT-proBNP assessed within 7 days before or after the CMR examination, alongside a CMR scan of sufficient image quality from which all sequences specified in our protocol could be completely obtained. The criteria for exclusion were delineated as follows: no serum NT-proBNP measurements conducted within 7 days before or after CMR imaging; the existence of CMR images exhibiting incomplete sequences, motion artifacts, or non-diagnostic quality attributable to technical or patient-related factors; and the lack of LGE images and ECV maps due to claustrophobia or contraindications for contrast agents.

The demographic data, clinical HF findings, history of previous medical conditions (hypertension, diabetes, renal failure), and serum NT-proBNP levels of the study cohort were recorded by searching the hospital database following the gathering of necessary permissions.

Cardiac magnetic resonance imaging protocol

All CMR examinations were performed utilizing a 1.5 T MRI scanner (Magnetom Aera; Siemens Medical Solutions, Erlangen, Germany) equipped with a phased-array (eight-channel) cardiac coil. All patients underwent a standardized CMR imaging protocol, generating structural and functional images, including native and contrast-enhanced T1 (for ECV calculation) and LGE. Imaging for each patient commenced with axial black-blood sequences, which was then followed by cine steady-state free precession (SSFP) sequences, conducted in either continuous short-axis or single-slice long-axis images (two-chamber, three-chamber, and four-chamber views) to evaluate chamber volume and function. In addition, T2-weighted short tau inversion recovery (STIR) images were obtained with the following parameters: repetition time (TR): 680 ms, echo time (TE): 69 ms, bandwidth: 836 Hz/pixel, matrix: 125 × 272, field of view: 360 × 275 mm, voxel: 1.3 × 1.3 × 6 mm^3, slice thickness: 6 mm, turbo factor: 20, and inversion time: 170 ms. Modified look-locker imaging (MOLLI) was utilized for T1 mapping, performed in a single mid-ventricular short-axis slice. Native T1 mapping was performed using a MOLLI 5(3)3 acquisition scheme, whereas post-contrast T1 mapping was performed using a MOLLI 4(1)3(1)2 acquisition scheme 10 minutes after contrast administration. Motion-corrected pixel-wise T1 maps were generated inline using the vendor-provided MyoMaps application (syngo MR E11E; Siemens Healthineers, Erlangen, Germany). Then, ECV maps were calculated from the corresponding native and post-contrast myocardial and blood-pool T1 values together with the same-day hematocrit measurements. Next, LGE was acquired about 15 minutes following an intravenous administration of 0.1 mmol/kg gadobutrol (Gadovist®, Bayer, Leverkusen, Germany), utilizing TR/TE: 9/3 ms, a flip angle of 25°, a voxel size of 1.3 × 1.3 × 6 mm, and an inversion duration ranging from 250 to 350 ms.

Image analyses

The CMR images were anonymized with respect to the patients' clinical data and were assessed by two radiologists with 15 and 8 years of expertise in cardiac imaging. The evaluation of cardiac structure and function was performed with commercially accessible software (syngo MR E11E, Siemens Healthcare, Erlangen, Germany).

The outlines of the left ventricle were manually delineated from short-axis balanced SSFP (bSSFP) images to ascertain end-diastolic volumes (EDVs) and end-systolic volumes (ESVs), as well as the left ventricular ejection fraction (LVEF), omitting the papillary muscles. Volume measurements were computed based on body surface area. Addi-

tionally, the LV myocardial volume was measured, and the myocardial mass was computed by multiplying this value by 1.05. Left ventricular wall thickness was assessed on end-diastolic short-axis cine bSSFP images at the mid-ventricular level. End-diastolic interventricular septal thickness and inferolateral wall thickness were measured perpendicular to the myocardial borders, excluding papillary muscles and trabeculations. The larger of these two measurements was used as the representative LV wall thickness for statistical analyses. The dimensions of the left atrium and ventricle were also documented.

The ECV was derived from a single mid-ventricular short-axis slice. Endocardial and epicardial contours were manually delineated on the native and post-contrast T1 maps, and a blood-pool region of interest (ROI) was placed within the LV cavity while avoiding papillary muscles and trabeculations. ECV was calculated using the following formula:

$$ECV\ (\%) = (1 - \text{hematocrit}) \times (\Delta R1\ \text{myocardium} / \Delta R1\ \text{blood}) \times 100,$$

where $\Delta R1 = (1/\text{post-contrast T1}) - (1/\text{native T1})$. The resulting value was reported as the mean mid-ventricular myocardial ECV, rather than the global myocardial ECV. However, LGE-positive regions were not excluded from the myocardial contour; therefore, the reported ECV represents a composite measure of focal and diffuse myocardial tissue abnormalities within the analyzed mid-ventricular slice and should not be interpreted as an isolated measure of diffuse interstitial expansion.

The presence and distribution of LGE were assessed visually using the standard 17-segment LV model. Each segment was assigned a semi-quantitative score according to the transmural extent of LGE: 0, no LGE; 1, 1%–25%; 2, 26%–50%; 3, 51%–75%; and 4, 76%–100% transmural involvement. The segment scores were summed and normalized to the maximum possible score of 68 using the following formula: (sum of segment scores/68) × 100. This segment-based percentage represents a semi-quantitative measure of LGE distribution and not the percentage of myocardial mass or volume occupied by a scar. Signal-thresholding methods, such as the 5-standard deviation or full-width at half-maximum technique, and planimetric scar quantification were not performed.

The STIR-based T2 signal-intensity (T2 SI) ratio was determined utilizing a standard T2-weighted black-blood turbo inversion recovery magnitude sequence acquired in short-axis planes. Measurements were obtained by manually positioning ROIs. For T2 SI assessment, endocardial and epicardial contours were manually delineated on five consecutive short-axis slices centered at the mid-ventricular level. The myocardial ROIs included the entire visible LV myocardium while excluding the blood pool, papillary muscles, and epicardial fat. Reference ROIs were placed within the serratus anterior muscle on three corresponding slices in which the muscle was clearly visualized, avoiding fascia, vessels, and artifacts. The mean myocardial SI was divided by the mean skeletal-muscle SI to calculate the T2 SI ratio. All ROI lines were conducted by the same radiologist, with agreement achieved through evaluation by a second radiologist collaborating with the first. This approach is conceptually based on the SI ratio method described in the original Lake Louise Criteria for CMR assessment of myocardial inflammation.[12] However, in the present study, the STIR-based T2 SI ratio was used solely as an exploratory non-contrast CMR parameter and was not applied as a diagnostic criterion for myocarditis.

Clinical data analysis

A third radiologist, blind to the CMR results, documented the demographic information and concomitant medical conditions of the patients in the research group. A fourth radiologist, unaware of both the medical records and the CMR results, documented the serum NT-proBNP levels taken within 7 days prior to and following the CMR scan date. Furthermore, the radiologists who conducted the measurements during the CMR examinations documented the etiological diagnoses (ischemic, hypertrophic, inflammatory, and infiltrative cardiomyopathies) associated with the patients' HF. The principal indication for CMR was obtained from the examination request form and electronic medical records. Final diagnoses were determined from the CMR report and the available clinical records. When more than one indication or diagnosis was present, the condition considered primarily responsible for the CMR examination or the principal imaging findings was used for classification. The distributions of CMR indications and final diagnostic categories are presented in Supplementary Table 1.

Statistical analysis

All analyses were performed using IBM SPSS Statistics 25.0 (IBM Corp., Armonk, NY, USA). Normality was assessed using the Kolmogorov–Smirnov test, and homogeneity of variances was evaluated using Levene's test. Continuous variables were presented as mean ± standard deviation or median (minimum–maximum), as appropriate. Group comparisons were performed using one-way analysis of variance or the Kruskal–Wallis test, with Dunn–Bonferroni post-hoc analysis when applicable. Categorical variables were expressed as frequencies and percentages and compared using the Pearson chi-square test or Fisher's exact test, as appropriate.

Because the NT-proBNP groups were naturally ordered, univariable ordinal logistic regression analyses were initially performed to evaluate the association between each CMR parameter and the increasing NT-proBNP group. The proportional-odds assumption was assessed using the test of parallel lines. Because this assumption was violated for ECV, a principal variable of interest, adjusted analyses were performed using multinomial logistic regression, which does not require the proportional-odds assumption. The normal NT-proBNP category (< 125 pg/mL) was used as the reference category, and separate odds ratios (ORs) were estimated for the high (125–500 pg/mL) and extremely high (> 500 pg/mL) groups. Multinomial logistic regression analysis was conducted to determine independent variables associated with escalating NT-proBNP categories. Clinically pertinent variables such as age, sex, hypertension, diabetes mellitus, chronic renal disease, and CMR-derived parameters were incorporated into the multivariable model. Adjusted ORs (aORs) with 95% confidence intervals (CIs) were reported. Model fit was assessed using likelihood ratio tests and pseudo R^2 statistics (Cox and Snell, Nagelkerke, and McFadden). Multicollinearity among predictors was evaluated using Pearson correlation coefficients prior to multivariable modeling. A two-sided P value < 0.05 was considered statistically significant.

Results

A total of 282 patients who had CMR scans during the designated 2-year period were identified. Sixty-five patients were excluded from the study due to the unavailability of serum NT-proBNP levels measured shortly prior to the CMR scan. Furthermore, the CMR images of 13 patients were excluded from the study due to non-compliance with the requisite criteria (artifact-laden images, lack of LGE or ECV images). A total of 204 patients who met the inclusion criteria were enrolled in the study. Figure 1 depicts the flowchart for patient selection and study inclusion.

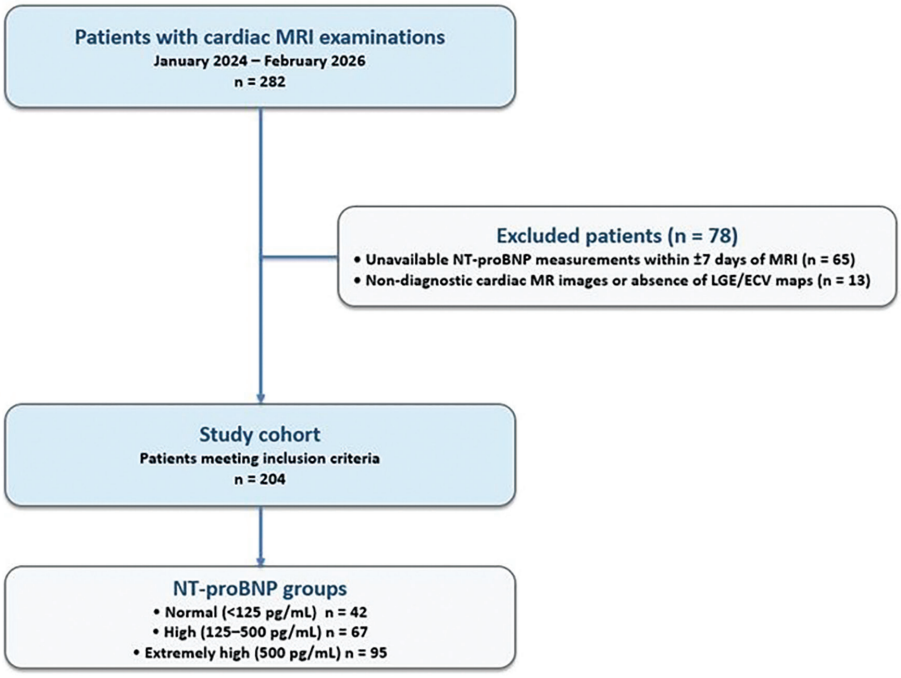

Figure 1. Flowchart of patient selection and study inclusion. MRI, magnetic resonance imaging; NT-proBNP, N-terminal pro-B-type natriuretic peptide; ECV, extracellular volume; LGE (%), LGE-positive left ventricular segments.

Of these patients, 128 (62.7%) were men and 76 (37.3%) were women. The median age was calculated as 53 (18–85) years.

We subsequently categorized the patients into three groups according to their serum NT-proBNP levels. Those with serum NT-proBNP levels below 125 pg/mL were included in the "normal" group, those in the range of 125–500 pg/mL in the "high" group, and those > 500 pg/mL in the "extremely high" group. The NT-proBNP levels utilized for categorization were established according to the existing literature.[4-6] We then compared LVEF, wall thickness, volume measurements, LGE data, and left atrial (LA) and LV cavity diameters from the CMR images among these three groups (Table 1).

Among our three patient groups, categorized by serum NT-proBNP levels, there were 42 patients (20.6%) in the normal group, 67 (32.8%) in the high group, and 95 (46.6%) in the extremely high group. The morphological and functional parameters evaluated in the CMR scans were compared among these three groups. Figure 2 shows the results for patients in the high group, and Figure 3 shows results for patients in the extremely high group; our evaluations are presented in the various sequences.

An analysis of the median patient age among the groups indicated that individuals in the high and extremely high NT-proBNP groups were older than those in the normal group, with *P* values of 0.004 and 0.001, respectively. No difference was observed between the high and extremely high serum NT-proBNP groups.

No significant difference was observed in the prevalence of comorbid conditions such as hypertension ($P = 0.872$), diabetes mellitus ($P = 0.921$), or chronic kidney disease ($P = 0.638$) among the NT-proBNP groups.

Upon comparison of median LVEF values among the groups, markedly lower LVEF values were noted in the extremely high group relative to the high and normal NT-proBNP groups. The *P* values were 0.03 and 0.001, respectively. No substantial difference was observed between the high and normal NT-proBNP groups ($P = 0.52$).

No difference in LV cavity diameter was observed among the three groups; however, a highly significant difference in LA cavity diameters was noted across all groups ($P < 0.001$).

The LGE%, defined as the proportion of segments demonstrating LGE relative to the total LV segments, was analyzed across the groups. Notably, LGE% demonstrated statistically significant differences among the three groups and correlated with elevated NT-proBNP levels ($P < 0.001$ for all groups) (Figure 4a).

The STIR-based T2 SI ratio, defined as the ratio of the mean SI values from the LV myocardium and the serratus anterior muscle, was compared across groups. The STIR-based T2 SI ratio exhibited statistically significant variations among the three groups and demonstrated a negative correlation with elevated NT-proBNP levels ($P < 0.001$ for all groups) (Figure 4b).

The ECV exhibited significant differences among all groups and demonstrated a robust positive correlation with serum NT-proBNP levels ($P < 0.001$) (Figure 4c).

Univariate ordinal logistic regression showed that LGE% (OR: 1.09 per one-unit increase, 95% CI: 1.03–1.15, $P = 0.005$), ECV (OR: 1.11 per one-unit increase, 95% CI: 1.04–1.18, $P < 0.001$), and LA cavity diameter (OR: 1.11 per one-unit increase, 95% CI: 1.05–1.18, $P < 0.001$) were positively associated with a higher NT-proBNP category. By contrast, the STIR-based T2 SI ratio was inversely associated with NT-proBNP category, with a 0.1-unit increase corresponding to a 15% reduction in the odds of being classified in a higher category (OR: 0.85, 95% CI: 0.76–0.96, $P = 0.008$).

In multivariable multinomial logistic regression analysis, ECV and LA cavity diameter were independently associated with the high NT-proBNP category compared with the normal group. In the extremely high NT-proBNP category, LGE%, ECV, STIR-based T2 SI ratio, and LA diameter remained independently associated. The inverse association of the STIR-based T2 SI ratio was restricted to the extremely high NT-proBNP group (OR: 0.80, 95% CI: 0.64–0.98, $P = 0.034$). Age, hypertension, diabetes mellitus, chronic kidney disease, LVEF, LV wall thickness, and myocardial volume were not independently associated with either NT-proBNP category in the multinomial model. The comprehensive model exhibited significant explanatory capability (likelihood ratio $P < 0.001$; McFadden pseudo R^2: 0.417).

Female sex was not associated with increasing NT-proBNP levels in the univariate ordinal logistic regression analysis. However, after multivariable adjustment, female sex was associated with both the high (aOR: 5.66, 95% CI: 1.61–19.86, $P = 0.007$) and extremely high NT-proBNP groups (aOR: 11.22, 95% CI: 2.53–49.81, $P = 0.001$), compared with the normal group, with male sex serving as the reference category.

The results of both the univariate (ordinal) and multivariate (multinomial) analyses are combined in Table 2.

Table 1. Clinical, demographic, and imaging characteristics of the patients

	Serum NT-proBNP levels			
	Normal (< 125 pg/mL)	High (125–500 pg/mL)	Extremely high (> 500 pg/mL)	*P* value
Patients n (%)	42 (20.6)	67 (32.8)	95 (46.6)	
Gender n (%)				
Men	31 (73.8)	35 (52.2)	62 (65.3)	
Women	11 (26.2)	32 (47.8)	33 (34.7)	
Age				
Median (min–max)	43 (18–66)	53 (18–79)	55 (18–85)	0.001
Mean ± SD	42.05 ± 14.8	52.1 ± 13.8	52.8 ± 15.4	
Comorbid conditions n (%)				
Hypertension	12 (28.6)	20 (29.9)	31 (32.6)	0.872
Diabetes mellitus	4 (9.5)	8 (11.9)	11 (11.6)	0.921
Chronic kidney disease	2 (4.8)	5 (7.5)	9 (9.5)	0.638
NT-proBNP level (pg/mL)				
Median (min–max)	46.5 (10–120)	254.8 (133–491)	1710 (501–35,000)	< 0.001
Mean ± SD	51.6 ± 36	271.9 ± 100.7	3,416.9 ± 5,339.4	
LVEDVi (mL/m^2)				
Median (min–max)	75.5 (35–124)	75 (34–184)	80 (17–266)	0.055
Mean ± SD	76.4 ± 19.2	78.9 ± 23.9	91.9 ± 41.1	
LVESVi (mL/m^2)				
Median (min–max)	28 (13–81)	30 (12–127)	35 (13–213)	0.015
Mean ± SD	31.4 ± 14.1	34.7 ± 19.8	48.6 ± 38.1	
LVEF				
Median (min–max)	63 (35–78)	61 (30–76)	58 (18–76)	< 0.001
Mean ± SD	61.4 ± 9.1	58.7 ± 10.2	52.2 ± 15	
LV wall thickness (mm)				
Median (min–max)	10 (6–24)	12 (7–22)	16 (6–34)	< 0.001
Mean ± SD	11.4 ± 3.6	12.7 ± 4	16.1 ± 5.7	
LV cavity diameter (mm)				
Median (min–max)	53 (34–71)	54 (38–72)	55 (16–92)	0.154
Mean ± SD	52.7 ± 6.1	54.8 ± 7.2	56 ± 10.8	
LV myocardial volume				
Median (min–max)	72 (57–138)	80 (46–186)	92 (55–290)	< 0.001
Mean ± SD	77.9 ± 18.3	82.5 ± 22.2	101.8 ± 37.1	
LV myocardial mass (g)				
Median (min–max)	76 (60–141)	84 (48–195)	97 (58–305)	< 0.001
Mean ± SD	81.9 ± 18.9	86.9 ± 23.2	107.2 ± 39	
Semi-quantitative LGE extent score (%)				
Median (min–max)	3 (0–17)	7 (0–30)	14 (0–53)	< 0.001
Mean ± SD	4.02 ± 4.1	8 ± 6.2	17.2 ± 12.8	
T2 ratio				
Median (min–max)	1.31 (0.48–1.98)	1.03 (0.52–1.9)	0.9 (0.28–2.21)	< 0.001
Mean ± SD	1.3 ± 0.3	1.1 ± 0.3	0.96 ± 0.29	
ECV (%)				
Median (min–max)	27 (24–35)	31 (24–53)	38 (26–62)	< 0.001
Mean ± SD	27.5 ± 3.1	32.8 ± 6.7	39.7 ± 8.8	
LA cavity diameter (mm)				
Median (min–max)	42.5 (30–50)	45 (35–60)	49 (34–92)	< 0.001
Mean ± SD	41.5 ± 4.6	45.3 ± 5.9	49.6 ± 7.9	

min–max, minimum–maximum; SD, standard deviation; LVEDVi, left ventricular end-diastolic volume index; LVESVi, left ventricular end-systolic volume index. Both parameters were indexed to body surface area (mL/m^2). The semi-quantitative LGE extent score was calculated as the sum of the 17 segmental transmurality scores divided by the maximum possible score of 68 and multiplied by 100. NT-proBNP, N-terminal pro-B-type natriuretic peptide; ECV, extracellular volume; LVEF, left ventricular ejection fraction; LA, left atrial; LV, left ventricular; LGE, late gadolinium enhancement.

Table 2. Univariate and multivariable associations between demographic, clinical, and cardiac MRI parameters with NT-proBNP groups

Variable	Univariate OR (95% CI)	*P*	High vs. normal aOR (95% CI)	*P*	Extremely high vs. normal aOR (95% CI)	*P*
Age	1.01 (0.98–1.03)	0.379	1.01 (0.97–1.05)	0.505	1.01 (0.96–1.05)	0.594
Female gender	1.04 (0.62–1.76)	0.876	5.66 (1.61–19.86)	0.007	11.22 (2.53–49.81)	0.001
Hypertension	1.16 (0.66–2.03)	0.602	0.91 (0.23–3.70)	0.905	0.33 (0.06–1.73)	0.192
DM	1.11 (0.49–2.50)	0.798	2.20 (0.32–14.87)	0.416	4.61 (0.54–19.1)	0.261
CKD	1.59 (0.60–4.26)	0.354	3.18 (0.31–12.05)	0.325	2.02 (0.14–18.8)	0.601
LGE (%)	1.09 (1.03–1.15)	0.005	1.11 (0.97–1.25)	0.117	1.18 (1.03–1.35)	0.013
T2 ratio	0.85 (0.76–0.96)	0.008	0.86 (0.72–1.02)	0.095	0.80 (0.64–0.98)	0.034
ECV (%)	1.11 (1.04–1.18)*	< 0.001	1.24 (1.07–1.45)	0.005	1.35 (1.15–1.59)	< 0.001
LVEF	0.96 (0.93–1.01)	0.071	0.98 (0.92–1.04)	0.651	0.95 (0.89–1.02)	0.188
LA diameter	1.11 (1.05–1.18)	< 0.001	1.15 (1.02–1.29)	0.012	1.25 (1.10–1.41)	0.001
LV wall thickness	1.10 (0.98–1.23)	0.092	0.99 (0.80–1.23)	0.985	1.12 (0.89–1.40)	0.330
LV myocard volume	1.01 (0.99–1.03)	0.098	1.01 (0.97–1.04)	0.541	1.02 (0.98–1.05)	0.196

Univariable associations were assessed using ordinal logistic regression. Adjusted associations were evaluated using multinomial logistic regression because the proportional-odds assumption was violated for ECV. The normal NT-proBNP group served as the reference group. Also, "Male" served as the reference for gender, and "no disease" was utilized as a reference for comorbid conditions. Odds ratios for the T2 ratio are reported per 0.1-unit increase, whereas those for all other continuous variables are reported per 1-unit increase. *Proportional-odds assumption violated in univariate ordinal model. NT-proBNP, N-terminal pro-B-type natriuretic peptide; MRI, magnetic resonance imaging; OR, odds ratio; aOR, adjusted odds ratio; CI, confidence interval; DM, diabetes mellitus; CKD, chronic kidney disease; LGE (%), late gadolinium enhancement-positive left ventricular segments (%); ECV, extracellular volume; LVEF, left ventricular ejection fraction; LA, left atrial; LV, left ventricular.

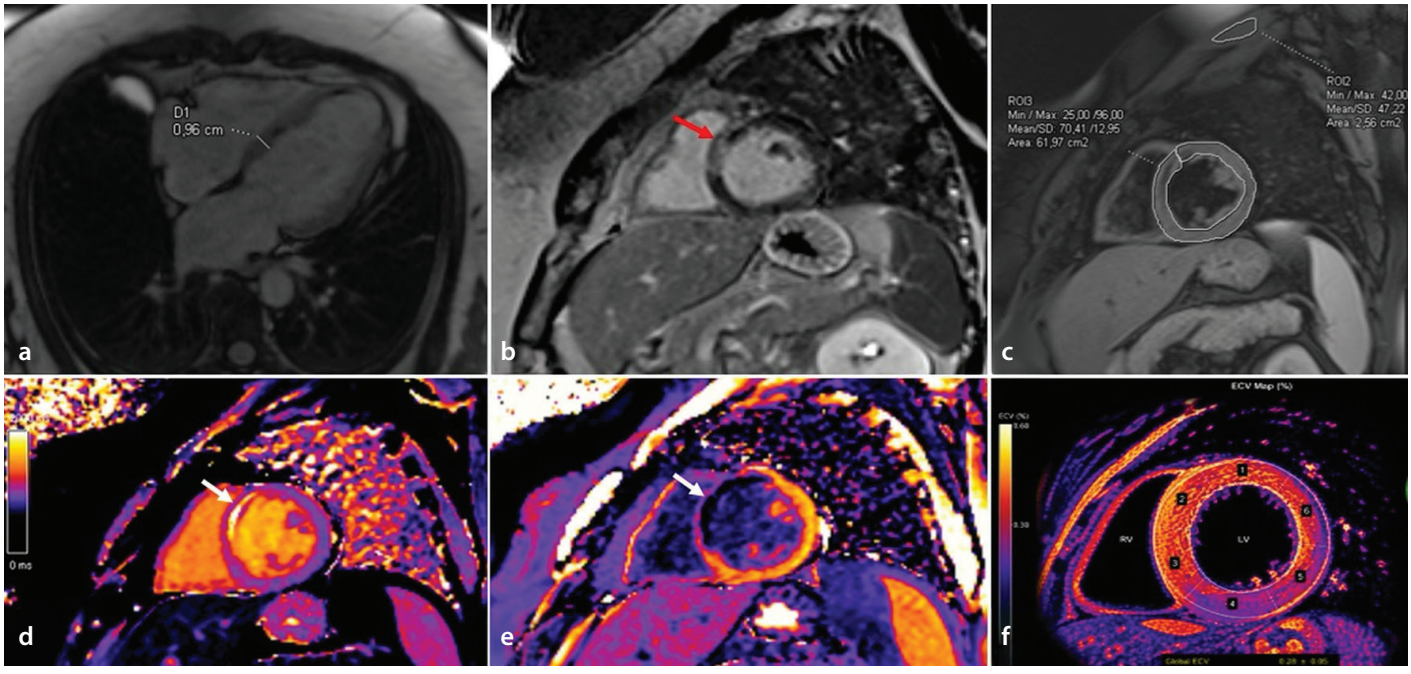

Figure 2. Cardiac magnetic resonance images of a 55-year-old male patient. The serum NT-proBNP concentration of the patient is 384 pg/mL, categorizing him in the high NT-proBNP group. **(a)** In the four-chamber long-axis cine image, where a marked reduction in left ventricular (LV) systolic function was noted, septal thickness was measured at 9.6 mm. **(b)** In late gadolinium enhancement images, subendocardial enhancement, extending in places to the mesocardial region, is noted in the septum and the free wall of the left ventricle (red arrow). **(c)** Myocardial and serratus muscle signal intensity was measured on T2-weighted turbo inversion recovery magnitude images. **(d)** Myocardial signal heterogeneity is observed on pre-contrast T1 mapping images (white arrow). **(e)** Relaxation changes consistent with contrast enhancement are noted on post-contrast T1 mapping images (white arrow). **(f)** On extracellular volume (ECV) mapping, a marked increase in ECV consistent with diffuse fibrosis and extracellular matrix expansion is observed, particularly in the affected segments. Overall, the findings are consistent with ischemic cardiomyopathy characterized by widespread fibrotic changes of ischemic origin and reduced LV function. NT-proBNP, N-terminal pro-B-type natriuretic peptide.

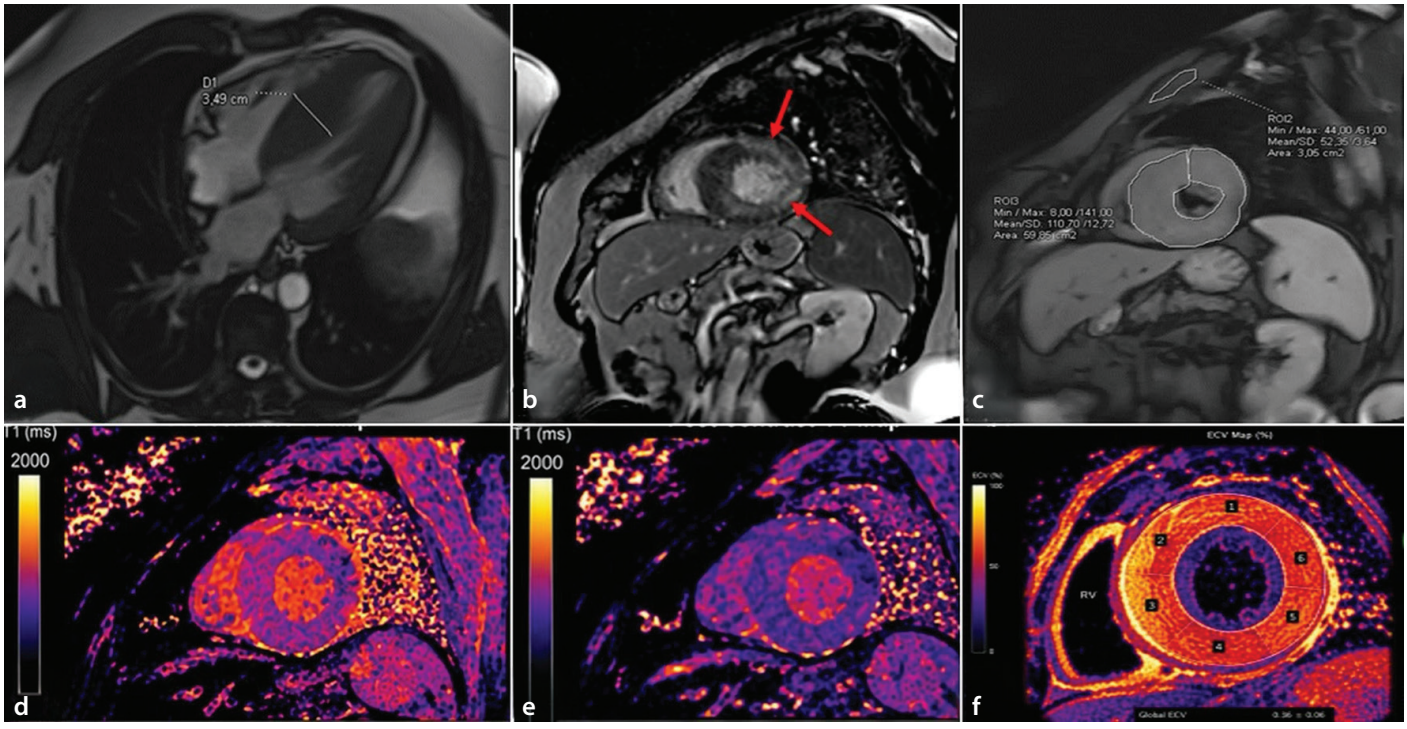

Figure 3. Cardiac magnetic resonance images of a 35-year-old male patient. The patient's serum NT-proBNP level is 1,241 pg/mL, placing him in the extremely high NT-proBNP group. **(a)** In the four-chamber long-axis cine image, increased end-diastolic interventricular septal thickness is observed (measurement lines: 34 mm). **(b)** In late gadolinium enhancement images, contrast enhancement is observed within the myocardium, particularly in the mesomyocardium (red arrows). **(c)** In the T2-weighted turbo inversion recovery magnitude image, global myocardial T2 signal intensity (SI) and the SI of the serratus muscle were measured. **(d)** Myocardial signal distribution is shown in the pre-contrast (native) T1 mapping image. **(e)** Myocardial changes are observed in the post-contrast T1 mapping image. **(f)** An increase in extracellular volume (ECV) consistent with myocardial extracellular matrix expansion, which is particularly evident in the septal region, was observed on the ECV map. Overall, the findings are consistent with a septal-predominant hypertrophic cardiomyopathy phenotype, with accompanying fibrotic changes and increased ECV being notable. NT-proBNP, N-terminal pro-B-type natriuretic peptide.

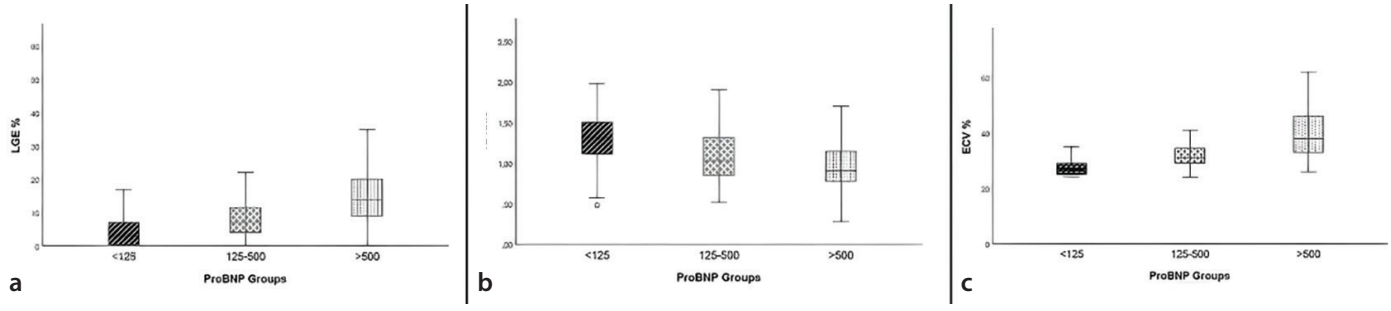

Figure 4. Boxplot showing median late gadolinium enhancement percentage **(a)**, T2 ratio **(b)**, and extracellular volume **(c)** values across various NT-proBNP groups. NT-proBNP, N-terminal pro-B-type natriuretic peptide.

Discussion

This study suggests elevated serum NT-proBNP levels correlate with a progressive deterioration in CMR findings, including conventional structural parameters and advanced tissue-characterization parameters. Higher NT-proBNP categories were associated with greater LV wall thickness, myocardial volume and mass, LA enlargement, lower LVEF, a higher proportion of LGE-positive segments, and an increased ECV. After adjustment for relevant covariates, ECV and LA cavity diameter were associated with both elevated NT-proBNP categories, whereas LGE% and the STIR-based T2 SI ratio were associated only with the extremely high category. The inverse association observed for the STIR-based T2 SI ratio should be interpreted cautiously. It may reflect differences in myocardial composition, disease stage, or the technical limitations of ratio-based measurements; however, the present observational findings cannot establish an underlying mechanism. Therefore, this result should be regarded as hypothesis-generating and requires confirmation in prospective studies.

Our findings endorse the perspective that NT-proBNP, as a biomarker, signifies not only hemodynamic stress but also the underlying structural and interstitial remodeling burden evident on CMR.[13-15] The expansion of LV wall thickness, myocardial volume, and myocardial mass, in conjunction with elevated NT-proBNP levels, aligns with progressive adverse remodeling. Specifically, although the LV cavity diameter exhibited no significant variation between groups, the LA diameter was markedly elevated across all categories. This pattern is significant, indicating that elevated NT-proBNP levels may more accurately or sensitively reflect chronic rises in filling pressures and diastolic load before noticeable ventricular cavity dilation occurs.[16] Elevation of this biomarker in this cohort seems to correlate with myocardial thickening, interstitial expansion, and atrial remodeling,

rather than merely geometric enlargement of the left ventricle. This helps to explain why the group with extremely high NT-proBNP has significantly lower LVEF values and why the transition to the high NT-proBNP group is characterized by tissue and atrial changes rather than marked systolic impairment.

Although female sex was not associated with increasing NT-proBNP levels in the univariable analysis, significant associations emerged for both elevated NT-proBNP groups after multivariable adjustment. This change may reflect confounding or a suppression effect related to differences in clinical and CMR characteristics between male and female patients. Nevertheless, the wide CIs indicate considerable uncertainty in the magnitude of these associations. Therefore, this finding should be interpreted cautiously and should not be considered evidence of a causal or sex-specific biological relationship. Confirmation in larger, prospectively designed cohorts with more balanced sex distributions is required.

An interesting finding was that although a significant association was observed between the LV ESV and NT-proBNP categories, only a borderline difference was detected between LV EDV and these categories. This pattern may reflect the closer relationship between NT-proBNP release and systolic dysfunction.

The correlation between NT-proBNP and LGE is among the most clinically significant result of this study. The presence of LGE suggests localized myocardial fibrosis, scarring, or infiltrative/replacement processes, depending on the characteristics of the underlying pathology.[17,18] The gradual increase in the proportion of LGE from the normal NT-proBNP group to the extremely high NT-proBNP group, along with its independent association in multivariate analysis, suggests that elevated natriuretic peptide levels are linked to a heightened extent of irreversible myocardial injury. This is especially significant, as NT-proBNP is often assessed exclusively in relation to volume or pressure overload.[19,20] Our data indicate that a substantial portion of the increase in NT-proBNP is attributable to the extent of structurally identified myocardial damage. Depending on the underlying etiology, LGE may represent myocardial fibrosis, scarring, or infiltrative/replacement processes.

Changes in pre- and post-contrast T1 values enable the evaluation of interstitial gadolinium concentration and ECV. In the absence of edema and amyloid accumulation, these measurements indicate extracellular matrix expansion correlated with elevated type I collagen levels, which contribute to stiffness. Moreover, ECV measurements have been shown to correlate with histological collagen volume fractions.[21] Since the ECV values obtained in our study were derived from overall myocardial measurements that also included regions showing LGE, the reported ECV values reflect the combined burden of focal and diffuse myocardial abnormalities rather than isolated interstitial remodeling. Among all the CMR imaging parameters, ECV emerged as the most dependable indicator correlated with NT-proBNP groups. The biological basis for this is that, in contrast to LGE—which is optimal for identifying focal fibrosis—ECV indicates extensive interstitial/extracellular expansion and thus may reveal earlier and more comprehensive myocardial remodeling.[22-24] The incremental rise in ECV among all NT-proBNP categories and its sustained presence in both the high and extremely high groups post-correction indicates a strong association between extensive extracellular matrix expansion and heightened natriuretic peptide levels. Thus, ECV may signify the imaging equivalent of chronic myocardial stress, manifesting before or alongside overt systolic failure. Of course, it should not be forgotten that these predictions were made without histopathological analysis data.

Future studies focusing on specific HF phenotypes, particularly HF with preserved EF, may further clarify the relationship between NT-proBNP and CMR-derived tissue-characterization markers.

The inverse association between the STIR-based T2 SI ratio and NT-proBNP represents an exploratory finding and should be interpreted cautiously. Myocardial edema in acute inflammatory or ischemic conditions is generally associated with increased SI on T2-weighted imaging.[12,25] However, our heterogeneous cohort was not restricted to patients with acute myocardial injury and included patients with different chronic cardiac conditions. Although changes in myocardial composition, fibrosis, or relative tissue water content might theoretically contribute to a lower STIR-based T2 SI ratio, these explanations remain speculative.

Importantly, the STIR-based T2 SI ratio was derived from conventional STIR-based SI measurements rather than quantitative T2 mapping. However, STIR-based measurements are susceptible to technical factors such as surface-coil sensitivity, sequence parameters, incomplete blood suppression, skeletal-muscle signal characteristics, and ROI placement. Therefore, the present study cannot determine whether the inverse association represents a true biological phenomenon or reflects technical characteristics of the imaging method. This finding should consequently be regarded as hypothesis-generating and not as evidence supporting the diagnostic or clinical use of the STIR-based T2 SI ratio. Validation using standardized quantitative T2 mapping, reproducibility analyses, and independent disease-specific cohorts is required.

This study suggests that LA cavity diameter is independently associated with NT-proBNP levels in this heterogeneous cohort. LA enlargement is widely recognized as a secondary indicator of persistently elevated LA filling pressure and diastolic load. Unlike instantaneous functional assessments, LA size reflects the cumulative effect of long-term hemodynamic stress.[26,27] This study suggests the independent correlation between LA diameter and NT-proBNP groups supports the view that elevated natriuretic peptides in HF are significantly associated with chronic pressure and volume overload rather than isolated ventricular systolic dysfunction. This finding underscores the synergistic importance of combining chamber remodeling measures with tissue-characterization indices in the CMR assessment of patients with HF.

Our study has several limitations. First, due to the retrospective nature of this single-center study, the generalizability of the findings is constrained. Another important limitation of this study is the clinical heterogeneity of the study population, which included patients with different underlying cardiac diseases. Myocardial tissue-characterization parameters may represent distinct pathological processes across ischemic, hypertrophic, inflammatory, and infiltrative cardiomyopathies. Therefore, differences in the distribution of disease etiologies may have influenced the observed associations between NT-proBNP and CMR parameters. Disease-specific subgroup analyses could not be performed because of the limited number of patients within several diagnostic categories. Accordingly, the findings should be interpreted as associations observed across a heterogeneous clinical cohort rather than as disease-specific relationships. Readers ought to proceed with vigilance in this matter. We recommend that future studies be designed to focus specifically on individual diseases. A further limitation relates to the utilization of NT-proBNP as the reference biomarker. Nota-

bly, NT-proBNP levels may exhibit significant physiologic and temporal variability, impacted by various factors unrelated to cardiac tissue properties, such as age, renal function, volume status, atrial arrhythmias, and current medical treatment. Although NT-proBNP is a recognized biomarker for assessing HF severity, a single measurement may inadequately represent the ongoing impact of myocardial remodeling. Consequently, the identified correlations must be understood in light of these possible confounding factors. Furthermore, LGE was assessed using a semi-quantitative segment-based method rather than quantitative signal-thresholding or planimetric techniques. Although this approach is practical and reflects the distribution of LGE-positive myocardial segments, it does not account for differences in scar size within individual affected segments. In addition, patients lacking contrast-enhanced images or ECV maps were excluded from the study, potentially introducing selection bias by omitting individuals with compromised renal function or more vulnerable clinical profiles. The T2 SI ratio was obtained from STIR SI measurements, which are inherently more vulnerable to technical variability than parametric mapping techniques and may be affected by imaging conditions, reference muscle characteristics, and ROI placement. Finally, as the outcome data were not analyzed, this study is unable to ascertain whether the identified CMR abnormalities correlate with the prognostic implications of NT-proBNP.

Our research contains several strengths. It assesses both conventional and advanced CMR parameters within the same cohort, employs a clinically relevant biomarker-based classification, and directly contrasts focal fibrosis and diffuse interstitial expansion using a conventional T2-weighted signal metric within a unified analytical framework. Multivariate modeling reinforces the assertion that the observed associations are not simply coincidental descriptive findings but indicate partially independent relationships between myocardial tissue characteristics and NT-proBNP levels.

In conclusion, increased NT-proBNP levels correlate with increasingly adverse CMR findings, encompassing more severe myocardial hypertrophy, LA remodeling, an augmented LGE burden, elevated ECV values, and an increased LA cavity diameter. Among these parameters, ECV demonstrated the strongest association with NT-proBNP severity, underscoring the pivotal role of extensive interstitial remodeling in patients with heightened natriuretic peptide levels. The inverse association observed between the STIR-based T2 ratio and extremely high NT-proBNP levels should be considered exploratory and hypothesis-generating. Because this measurement may be influenced by technical factors and was not based on quantitative T2 mapping, further studies using standardized parametric mapping and reproducibility assessment are required before any biological or clinical significance can be established.

Footnotes

Conflict of interest disclosure

The authors declared no conflicts of interest.

Supplementary Table: https://d2v96fxpocvxx.cloudfront.net/2c83d69a-dc5a-476c-9385-2d943ca48693/content-images/17117ddd-6065-4034-b99d-b525976a4488.pdf

References

1. Mueller C, McDonald K, de Boer RA, et al. Heart Failure Association of the European Society of Cardiology practical guidance on the use of natriuretic peptide concentrations. *Eur J Heart Fail*. 2019;21(6):715-731. [Crossref]
2. Zhao X, Li H, Liu C, Ren Y, Sun C. NT Pro-BNP can be used as a risk predictor of clinical atrial fibrillation with or without left atrial enlargement. *Clin Cardiol*. 2022;45(1):68-74. [Crossref]
3. Hendricks S, Dykun I, Balcer B, Totzeck M, Rassaf T, Mahabadi AA. Higher BNP/NT-pro BNP levels stratify prognosis equally well in patients with and without heart failure: a meta-analysis. *ESC Heart Fail*. 2022;9(5):3198-3209. [Crossref]
4. Bayes-Genis A, Docherty KF, Petrie MC, et al. Practical algorithms for early diagnosis of heart failure and heart stress using NT-proBNP: a clinical consensus statement from the Heart Failure Association of the ESC. *Eur J Heart Fail*. 2023;25(11):1891-1898. [Crossref]
5. Pellicori P, Cleland JGF. Structural heart disease, cardiac dysfunction and heart failure: the ambiguity of a definition. *Eur J Prev Cardiol*. 2021;28(9):921-923. [Crossref]
6. Mouzarou A, Hadjigeorgiou N, Melanarkiti D, Plakomyti TE. The role of NT-proBNP levels in the diagnosis of hypertensive heart disease. *Diagnostics (Basel)*. 2025;15(1):113. [Crossref]
7. Pan J, Ng SM, Neubauer S, Rider OJ. Phenotyping heart failure by cardiac magnetic resonance imaging of cardiac macro- and microscopic structure: state of the art review. *Eur Heart J Cardiovasc Imaging*. 2023;24(10):1302-1317. [Crossref]
8. Kramer CM, Barkhausen J, Bucciarelli-Ducci C, Flamm SD, Kim RJ, Nagel E. Standardized cardiovascular magnetic resonance imaging (CMR) protocols: 2020 update. *J Cardiovasc Magn Reson*. 2020;22(1):17. [Crossref]
9. Messroghli DR, Moon JC, Ferreira VM, et al. Correction to: Clinical recommendations for cardiovascular magnetic resonance mapping of T1, T2, T2* and extracellular volume: a consensus statement by the Society for Cardiovascular Magnetic Resonance (SCMR) endorsed by the European Association for Cardiovascular Imaging (EACVI). *J Cardiovasc Magn Reson*. 2018;20(1):9. [Crossref] Erratum for: *J Cardiovasc Magn Reson*. 2017;19(1):75. [Crossref]
10. Yang EY, Khan MA, Graviss EA, et al. Relationship of extracellular volume assessed on cardiac magnetic resonance and serum cardiac troponins and natriuretic peptides with heart failure outcomes. *Sci Rep*. 2019;9(1):20168. [Crossref]
11. Rahsepar AA, Bluemke DA, Habibi M, et al. Association of pro-B-type natriuretic peptide with cardiac magnetic resonance-measured global and regional cardiac function and structure over 10 years: the MESA study. *J Am Heart Assoc*. 2021;10(8):e019243. [Crossref]
12. Ferreira VM, Schulz-Menger J, Holmvang G, et al. Cardiovascular magnetic resonance in nonischemic myocardial inflammation: expert recommendations. *J Am Coll Cardiol*. 2018;72(24):3158-3176. [Crossref]
13. Liu CY, Heckbert SR, Lai S, et al. Association of elevated NT-proBNP with myocardial fibrosis in the Multi-Ethnic Study of Atherosclerosis (MESA). *J Am Coll Cardiol*. 2017;70(25):3102-3109. [Crossref]
14. Assadi H, Matthews G, Chambers B, et al. Cardiac magnetic resonance left ventricular filling pressure is associated with NT-proBNP in patients with new onset heart failure. *Medicina (Kaunas)*. 2023;59(11):1924. [Crossref]
15. Li Y, Liu J, Cao Y, et al. Predictive values of multiple non-invasive markers for myocardial fibrosis in hypertrophic cardiomyopathy patients with preserved ejection fraction. *Sci Rep*. 2021;11(1):4297. [Crossref]
16. Blanco R, Ambrosio G, Belziti C, et al. Prognostic value of NT-proBNP, and echocardiographic indices of diastolic function, in hospitalized patients with acute heart failure and preserved left ventricular ejection fraction. *Int J Cardiol*. 2020;317:111-120. [Crossref]
17. Giordano C, Francone M, Cundari G, Pisano A, d'Amati G. Myocardial fibrosis: morphologic patterns and role of imaging in diagnosis and prognostication. *Cardiovasc Pathol*. 2022;56:107391. [Crossref]
18. Disertori M, Rigoni M, Pace N, et al. Myocardial fibrosis assessment by LGE is a powerful predictor of ventricular tachyarrhythmias in ischemic and nonischemic LV dysfunction:

a meta-analysis. *JACC Cardiovasc Imaging*. 2016;9(9):1046-1055. [Crossref]

19. de la Espriella R, Cobo M, Santas E, et al. Assessment of filling pressures and fluid overload in heart failure: an updated perspective. *Rev Esp Cardiol (Engl Ed)*. 2023;76(1):47-57. [Crossref]
20. Tschöpe C, Kasner M, Westermann D, et al. Elevated NT-ProBNP levels in patients with increased left ventricular filling pressure during exercise despite preserved systolic function. *J Card Fail*. 2005;11(5 Suppl):S28-S33. [Crossref]
21. Haaf P, Garg P, Messroghli DR, Broadbent DA, Greenwood JP, Plein S. Cardiac T1 mapping and extracellular volume (ECV) in clinical practice: a comprehensive review. *J Cardiovasc Magn Reson*. 2016;18(1):89. [Crossref]
22. Meier C, Eisenblätter M, Gielen S. Myocardial late gadolinium enhancement (LGE) in cardiac magnetic resonance imaging (CMR)-an important risk marker for cardiac disease. *J Cardiovasc Dev Dis*. 2024;11(2):40. [Crossref]
23. Lurz JA, Luecke C, Lang D, et al. CMR-derived extracellular volume fraction as a marker for myocardial fibrosis: the importance of coexisting myocardial inflammation. *JACC Cardiovasc Imaging*. 2018;11(1):38-45. [Crossref]
24. Gao Y, Wang HP, Liu MX, et al. Early detection of myocardial fibrosis in cardiomyopathy in the absence of late enhancement: role of T1 mapping and extracellular volume analysis. *Eur Radiol*. 2023;33(3):1982-1991. [Crossref]
25. Pan JA, Lee YJ, Salerno M. Diagnostic performance of extracellular volume, native T1, and T2 mapping versus lake louise criteria by cardiac magnetic resonance for detection of acute myocarditis: a meta-analysis. *Circ Cardiovasc Imaging*. 2018;11(7):e007598. [Crossref]
26. Thomas L, Marwick TH, Popescu BA, Donal E, Badano LP. Left atrial structure and function, and left ventricular diastolic dysfunction: JACC state-of-the-art review. *J Am Coll Cardiol*. 2019;73(15):1961-1977. [Crossref]
27. Rosca M, Lancellotti P, Popescu BA, Piérard LA. Left atrial function: pathophysiology, echocardiographic assessment, and clinical applications. *Heart*. 2011;97(23):1982-1989. [Crossref]